Macromolecules **2009**, *42*, 1175–1179

A New Facile Method for Preparation of Nylon-6 with High Crystallinity and Special Morphology

Huizhen Li,[†,‡] Yanjie Wu,[§] Harumi Sato,[||] Lei Kong,[§] Chengfeng Zhang,[§] Kun Huang,[†] Dongliang Tao,[†] Jing Chen,[†] Xuexin Liu,[§] Ying Zhao,[§] Yizhuang Xu,[*,†] Jinguang Wu,[†] and Yukihiro Ozaki[||]

College of Chemistry and Molecular Engineering, Peking University, Beijing 100871, P. R. China, College of Chemistry and Environmental Science, Henan Normal University, Xinxiang, 453007, P. R. China, Institute of Chemistry, Chinese Academy of Sciences, Beijing 100080, P. R. China, and Department of Chemistry, School of Science and Technology, Kwansei-Gakuin University, Sanda, 669-1337, Japan

Received August 26, 2008; Revised Manuscript Received December 23, 2008

ABSTRACT: In this study, we develop a new facile method to prepare nylon-6 with special features (denoted as vp-nylon-6). The key strategy for the method is to make the crystallization of nylon-6 be performed in a slow and near-equilibrium manner by diffusing the vapor of precipitator into a nylon 6/formic acid solution at ambient temperature and pressure. Differential scanning calorimeter (DSC) and wide angle X-ray diffraction (WAXD) have demonstrated that the crystallinity and crystalline perfection of vp-nylon-6 are significantly improved by the new method. Scanning electron microscope (SEM) observations have shown that vp-nylon-6 exhibits versatile morphological features including ribbon, bowknot, flower, semisphere, and dumbbell which are the result of the assembly of crystalline lamellae. The crystalline lamellae occur in a discrete fashion rather than being embedded in an amorphous matrix even if concentrated nylon solutions are used. Selected area electron diffraction (SAED) in transmission electron microscope (TEM) shows that the crystalline lamellae are composed of single crystals.

1. Introduction

Linear aliphatic polyamides, commonly known as nylon, occupy a prominent position in the realm of polymers.[1] Nylon usually exhibits high modulus, toughness and strength, low creep and good temperature resistance that allow nylon wide applications including fibers and engineering thermoplastics.[1–4] Moreover, nylon is an attractive carrier and has great potential in bioengineering involving protein immobilization since it has amide groups in the main chain.[5–9] In this aspect, nylon with special structure and morphology possesses bright perspective and advantage in developing bioreactors with superior performance.

It is generally recognized that macroscopic properties of semicrystalline polymers are governed by their microscopic structural features such as crystalline structure, morphology, which in turn, are closely related to the processing methods. Therefore, a considerable number of studies have been carried out to explore the crystallization behavior and morphology of nylon-6 from solutions and melts.[10–54] Several research groups reported the new methods to prepare nylon with special structures and/or morphologies. Pei synthesized nylon microspheres with designed morphology by adjusting phase inversion morphology generated in the nylon-6/polystyrene blends at very low PS contents.[42] Crespy prepared Nylon 6 nanoparticles and nanocapsules by two novel miniemulsion/solvent displacement hybrid techniques.[43] Tonelli successfully manipulated polymorphic crystal structures, crystallinity, and orientation of nylon-6 by using nylon-6/α-cyclodextrin inclusion complex.[44,45] Cai observed scrolled and tubular lamellar crystals of nylon-66 through self-seeding solution crystallization.[26]

In nylon-6, strong hydrogen bondings are formed among adjacent polymer chains in both crystalline and amorphous regions. The hydrogen bonds act as quasi-cross-links, inhibiting the sliding of the polymer chain cross the hydrogen-bonding plane. Consequently, the nylon chains often stop in meta-stable state during the crystalline procedure. Thus, the crystallinity of nylon-6 cannot be very high after conventional treatments. A typical crystallinity of nylon-6 is about 30%.

In a nylon-6 solution, a solvating layer is formed around each polymer chain. The solvating layer alleviates molecular entanglement and weakens hydrogen bonds among neighboring nylon chains considerably, and thus the polymer chain can move more freely. During the crystalline process, it is much easier for the polymer to attain a stable and order structure as the solvating layer is deprived gradually and the polymer chains are packed together.

Considering nylon-6 dissolved in formic acid, it will precipitate from the solution when precipitator such as water, THF, methanol, ethanol, etc., is added. In our previous work, we found that the crystallinity of polymeric materials is governed by the speed of crystallization.[55,56] Thus, we have developed a new facile method to prepare nylon-6 with special features by diffusing the vapor of precipitator into a nylon-6/formic acid solution so that the crystallization can be performed in a slow and near-equilibrium manner at ambient temperature and pressure. We have named the nylon-6 thus prepared vp-nylon-6. It has been found that vp-nylon-6 exhibits high crystallinity and versatile morphological features.

2. Experimental Section

A nylon-6 ($M_r = 2.65 \times 10^4$)/formic acid solution and a reservoir of precipitator of nylon-6, such as water, ethanol, methanol, THF etc., were put in a sealed container. As the time elapses, the precipitator evaporates into the air of the sealed container and diffuses into the nylon-6 solution, inducing the crystallization of nylon-6. The process of crystallization can be adjusted by the speed of introducing the vapor of the precipitator into the nylon-6 solution,

---

[*] Corresponding author. E-mail: xyz@pku.edu.cn.

[†] College of Chemistry and Molecular Engineering, Peking University.

[‡] College of Chemistry and Environmental Science, Henan Normal University.

[§] Institute of Chemistry, Chinese Academy of Sciences.

[||] Department of Chemistry, School of Science and Technology, Kwansei-Gakuin University.

10.1021/ma8019333 CCC: $40.75

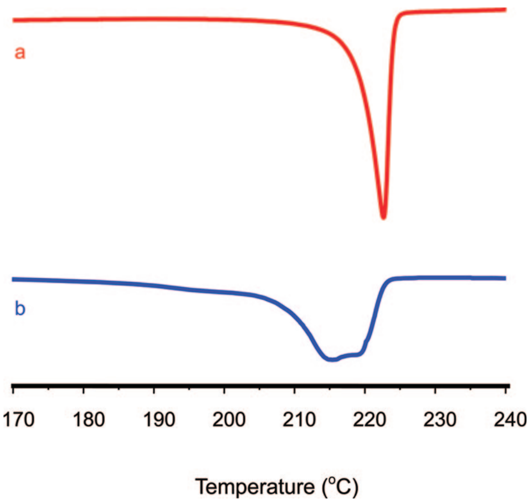

Figure 1. DSC thermograms of nylon-6: (a) vp-nylon-6; (b) gt-nylon-6.

which can be achieved by adjusting the environmental temperature of the liquid precipitator. Sometimes a formic acid reservoir was also put in the sealed container to compensate for the loss of solvent from the nylon-6 solution.

In our experiment, the optimized environmental temperature was 21 °C and the concentration of nylon-6 can be 10 wt %. It took about 1−2 weeks to complete the crystallization process. The resultant vp-nylon-6 powder was filtered, washed with THF, acetone and dried in the open air. For comparison, another nylon-6 sample was prepared by using general thermal treatment processes (denoted as gt-nylon-6). That is, the nylon-6 sample was melted and kept at 280 °C for 15 min and then cooled down slowly to induce the crystallization at a cooling rate of 1 °C/min.

The DSC experiments were carried out on a TA Q100 DSC Instruments. The scanning rate was 10^{o}C/min. WAXD measurements of the vp-nylon-6 and gt-nylon-6 samples were performed on a Rigaku D/MAX-RB wide-angle X-ray diffractometer.

The morphology of the vp-nylon-6 samples was also examined by using a Hitachi H800 transmission electronic microscope and a JEOL 6700F scanning electronic microscope.

3. Results and Discussion

Crystallinity and Crystalline Perfection. The DSC thermograms for a typical vp-nylon-6 and a typical gt-nylon-6 sample are plotted in Figure 1. Remarkable differences between the two samples can clearly be observed. The DSC trace of the vp-nylon-6 sample exhibits only a sharp melting peak. The melting peak of the gt-nylon-6 sample has a shape of a wide envelope that is attributed to the superposition of multiple melting and premelting processes. The melting enthalpies of vp-nylon-6 samples are between 110 and 163 J/g, while those melting enthalpies gt-nylon-6 samples are only between 60−90 J/g. The higher melting enthalpies of vp-nylon-6 samples indicate that they have higher crystallinity. The sharp, single melting peak of the vp-nylon-6 sample shows that the thickness of the crystalline lamellae is within a narrow range. The absence of the premelting phenomenon suggests that there are little metastable nylon crystallites in the vp-nylon-6 samples. The feature of DSC thermogram of the vp-nylon-6 sample is partially similar to that of the coalesced nylon-6 prepared by using nylon-6/α-cyclodextrin inclusion complex where sharp melting peak can be observed.[45]

Parts a−c of Figure 2 show WAXD patterns of three kinds of nylon 6 samples: gt-nylon, vp-nylon-6, and vp-nylon-6 in a special case. Two diffraction peaks at about 20° and 24°, which are assigned to the (200) and (002/202) reflections of α nylon-6, respectively,[10] can be observed. It is clear that no γ phase occurs since the characteristic peak at 21° is not observable.[19] In both vp-nylon-6 and gt-nylon-6 samples, amorphous nylon occurs and exhibits a broad halo around 22°. We have used curve fitting simulation on the X-ray diffraction curves to estimate the crystalline contents of the gt-nylon-6 and vp-nylon-6 samples. The calculation in detail can be found in the supplement materials. The results demonstrate that the vp-nylon-6 sample exhibits higher crystallinity. The pattern of XRD of the vp-nylon-6 sample is partially similar to that of the coalesced nylon-6 prepared by using nylon-6/α-cyclodextrin inclusion complex where α nylon-6 dominate and significantly increase in crystallinity is observed.[45]

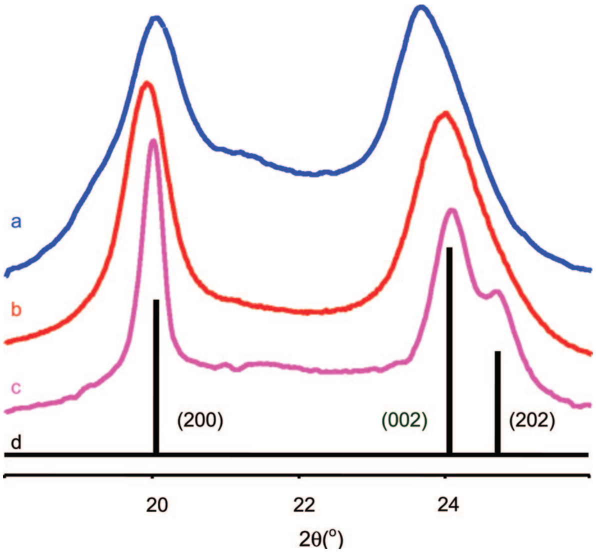

Figure 2. WAXD patterns of nylon-6: (a) gt-nylon-6; (b) vp-nylon-6; (c) the vp-nylon-6 sample in a special case d simulated WAXD of nylon-6 in α form.

Moreover, the separation in peak positions between the two crystalline peaks at 20° and 24° is larger for the vp-nylon-6 in comparison with that of the gt-nylon-6. According to the literature,[31,51] the increase in the separation between the two above reflections represents an energetically lower and more stable α nylon-6 lattice. That is to say, the perfection of the vp-nylon-6 crystallites is improved significantly.

Additionally, the widths of diffraction peaks of most of vp-nylon-6 samples decrease in comparison with those of the gt-nylon-6 sample, indicating that the size of crystallites increases considerably in the vp-nylon-6. The Scherrer analysis[57] was performed on the peak width of the (200) reflection peak obtained by curve fit calculation (The peak widths are listed in the Supporting Information). The average crystallite size for the (200) reflection is 8.7 nm for the gt-nylon 6 sample and 11.0 nm for the vp-nylon-6 sample, respectively. A drastic decrease in the width of the diffraction peak can be observed in some special vp-nylon-6 samples (Figure 2c). The corresponding size of the crystallites for the (200) reflection amounts to 23.2nm.

The decrease in the diffraction peak widths can also be manifested by a marked change in the diffraction peak at 24°. According to the simulated WAXD pattern based on the crystal structure of nylon 6 in α form,[10] the 24° peak is actually composed of a strong peak for (002) reflection at 24.0° and a weak peak for (202) reflection at 24.8° (Figure 2d). According to the experimental results reported in the literature[29,31−33,41,45] or in our previous work,[55,58] the overlapping of the two peaks at 24° and 24.8° is so severe that it is almost impossible to resolve individual subpeak from the overlapping envelop. However, the diffraction peak for (002) and (202) reflections

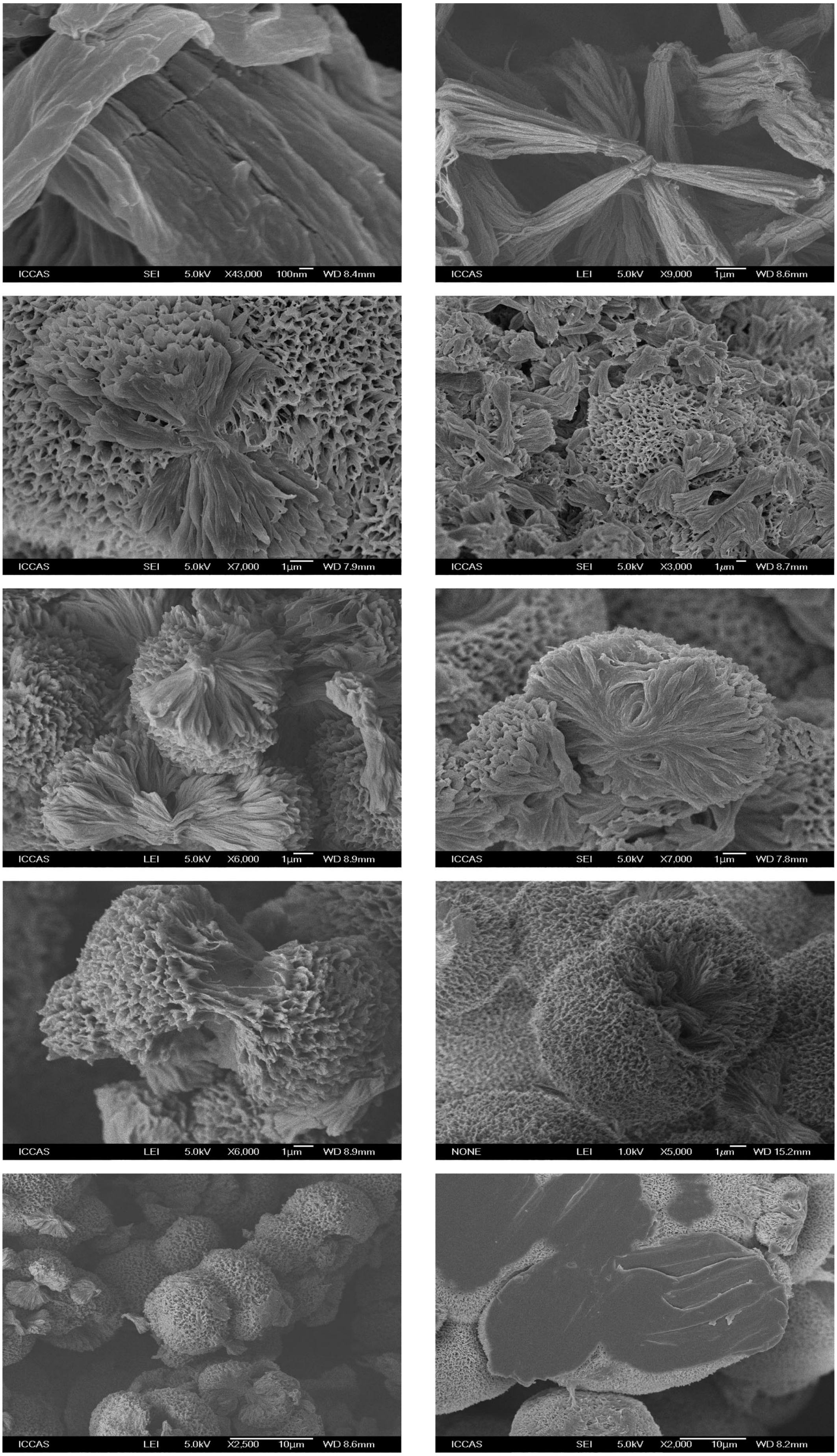

Figure 3. SEM images of vp-nylon-6 with various morphologies.

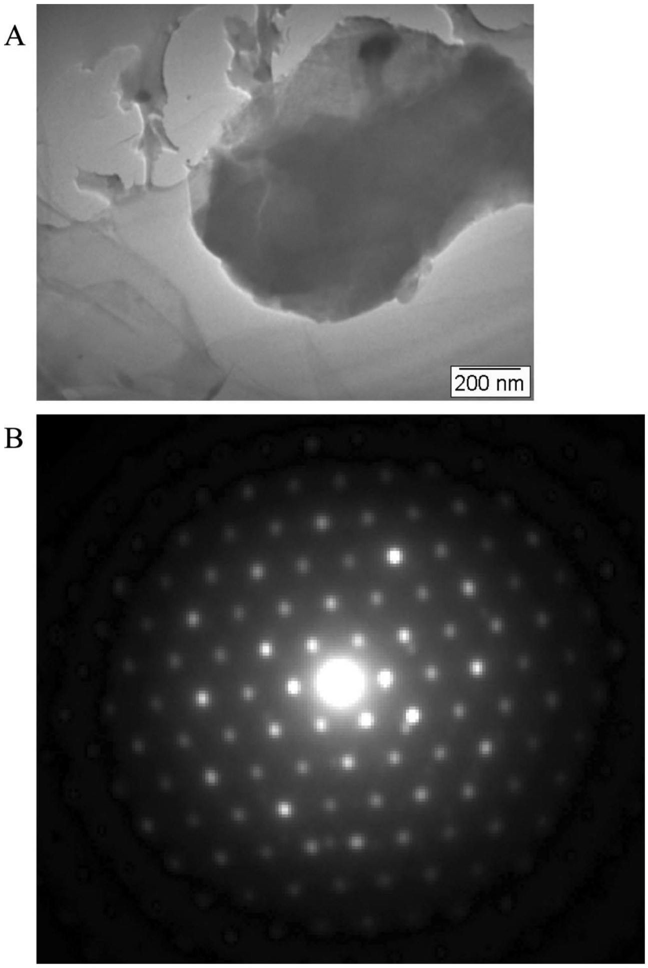

Figure 4. (A) TEM micrograph of a vp-nylon-6 lamella. (B) SAED of the vp-nylon-6 lamella.

can be directly observed for the aforementioned vp-nylon-6. In summary, the WAXD results show that the vp-nylon-6 samples hold high crystallinity and improved crystalline perfection. In some cases, nylon-6 with larger crystallites can be obtained by using the vapor precipitation method (Figure 2c).

Morphological Characterization. To enhance our understanding of the crystalline behavior of nylon-6 by using the vapor precipitation approach, SEM experiment was also performed. The vp-nylon-6 sample exhibit versatile morphological features as shown in Figure 3. Although the shapes of vp-nylon-6 are different from sample to sample, a common structural feature can be observed. That is, vp-nylon-6 is the assembling of discrete lamellae into complex architectures such as ribbon, bowknot, hemisphere, double-hemisphere, flower, etc. In some cases, flat lamellae may form stack assembly. The thickness of the lamellae is estimated to be less than 10 nm. The high crystallinity of the vp-nylon-6 samples observed by DSC and WAXD in the previous part suggests that the lamellae are composed of crystalline nylon. To verify whether the lamella is crystalline or not, we utilized selected area electronic diffraction (SAED) in TEM to study the nylon lamella. A typical TEM image and an SAED pattern are shown in Figure 4. The lamella turns out to be single crystal since diffraction spots can be observed. Thus, we conclude that the vp-nylon-6 samples are the assembly of discrete crystalline nylon lamellae.

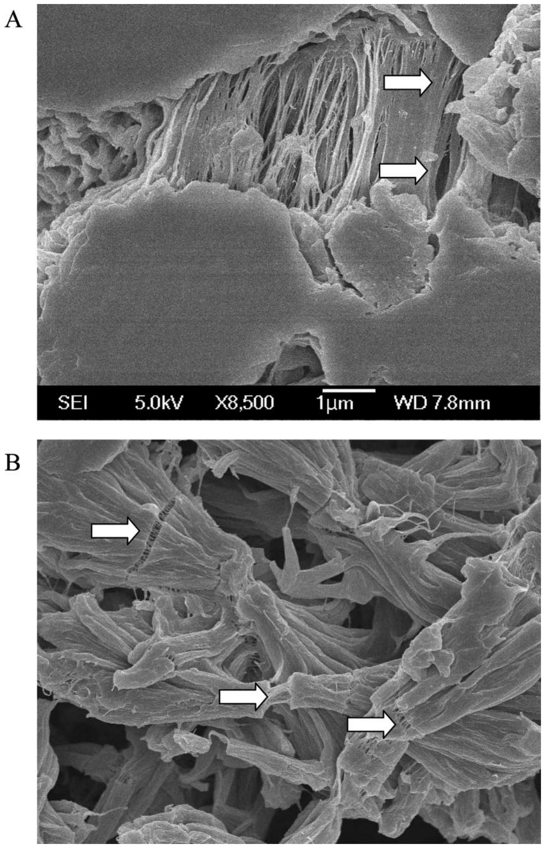

Figure 5. (A) First type of cracking with smooth and clear cutting edges. (B) Second type of cracking with fibrillar linkages.

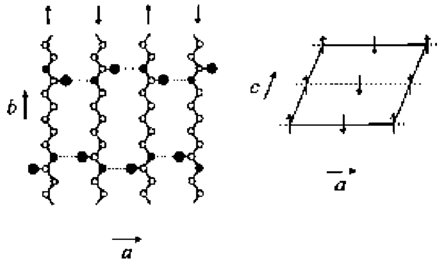

Figure 6. Structure of nylon 6 in the α-phase.

An interesting phenomenon is that the crystalline lamella of the vp-nylon-6 sample exhibits complex cracking behavior. The crack of the nylon crystalline lamella can be classified into two types (Figure 5). The first type of cracking holds the feature that the nylon lamella is cleaved with smooth and clear cutting edges (Figure 5A). In the second type of cracking, the breaking lamella is not completely separated but connected by fibrillar materials perpendicular to the breaking edge of nylon (Figure 5B).

The above phenomenon is related to the anisotropy of crystalline lamella in α form and the folded chain model proposed by Keller.[59] The structure of nylon 6 in the α-phase is illustrated in Figure 6.[10] Within the crystal lattice, hydrogen bonds form between antiparallel chains of nylon 6 in all-trans chain conformations, constituting a hydrogen-bonded sheet. As a result, van der Waals interactions are left to combine adjacent hydrogen-bonded sheets. The weak linkage makes it easy to cleavage nylon-6 lamella between adjacent hydrogen-bonded sheets. This is the reason why smooth and clear cleavage plane can be observed in the first type of cracking lamella.

The observation of fibrillar materials across the cutting edge may be explained according to the Keller's model.[59] When a crystalline lamella breaks into two parts, two polymer segments embedded in different parts of the lamellae may be linked by a hairpin-like polymer chain on the surface of crystalline lamellae. It is almost impossible to break the hairpin-like chain since it involves the breaking of chemical bonds. Consequently, the socalled breaking lamella is not completely cracked but linked by polymer chains that form fibrillar materials striding across the breaking lamellae.

4. Conclusions

In the present study, we allow the vapor of the precipitator of nylon to diffuse into a nylon-6/formic acid solution so that the crystallization of nylon 6 can be performed in a slow and near-equilibrium manner. It can be seen from DSC and WAXD measurement that the obtained nylon (vp-nylon-6) is dominated by stable α modification with superior crystallinity and crystalline perfection. SEM and TEM results demonstrate that vp-nylon-6 exhibits versatile morphology whose building block is discrete crystalline lamella. A noticeable feature of the approach described in this paper is that the crystalline lamella is not embedded by an amorphous matrix even if a concentrated solution (10 wt %) is used. For comparison, discrete crystalline lamellae can only be obtained by crystallization of polymer from a dilute solution with careful control of experimental condition in the literature. Therefore, this approach provides an effective method to prepare large amount of crystalline lamella of nylon-6.

Acknowledgment. This project was supported by the National Natural Science Foundation of China (NSFC50673005, NSFC50403026, NSFC20671007). This work was partially supported by "Open Research Center" project for private Universities: matching fund subsidy from MEXTn (Ministry of Education, Culture, Sports, Science and Technology), 2001−2008. This work was support also by Kwansei-Gakuin University "Special Research" Project, 2004−2008, China Postdoctoral Science Foundation funded project: 200801007; 20070410002.

Supporting Information Available: Text giving the results of curve fit simulation on X-ray diffraction curves, figures showing the curve fitting results and Tables S1 and S2. This material is available free of charge via the Internet at http://pubs.acs.org.

References and Notes

(1) Zhang, C. G.; Liu, M. Y.; Zhao, Q. X.; Wang, Y. D.; Liu, S. T. *J. Appl. Polym. Sci.* **2003**, *89*, 379–385.
(2) Muratoğlu, O. K.; Argon, A. S.; Cohen, R. E. *Polymer* **1995**, *36*, 2143–2152.
(3) Penel, L.; Depecker, C.; Séguéla, R.; Lefebvre, J.-M. *J Polym Sci., Polym Phys* **2001**, *39*, 484–495.
(4) Kotek, R.; Jung, D.; Tonelli, A. E.; Vasanthan, N. *J. Macromol., Sci., Part C: Polymer Reviews* **2005**, *45*, 201–230.
(5) Beeskow, T. C.; Kroner, K. H.; Anspach, F. B. *J. Colloid Interface Sci.* **1997**, *196*, 278–291.
(6) Yalcüin, G.; Elmas, B.; Tuncel, M.; Tuncel, A. *J. Appl. Polym. Sci.* **2006**, *101*, 818–824.
(7) Hu, J.; Li, S. J.; Liu, B. L. *Biotechnol. J.* **2006**, *1*, 75–79.
(8) Jia, X. Q.; Herrera-Alonso, M.; McCarthy, T. J. *Polymer* **2006**, *47*, 4916–4924.
(9) Herrera-Alonso, M.; McCarthy, T. J.; Jia, X. Q. *Langmuir* **2006**, *22*, 1646–1651.
(10) Holmes, D. R.; Bunn, C. W.; Smith, D. J. *J. Polym. Sci.* **1955**, *17*, 159–177.
(11) Tsuruta, M.; Arimoto, H.; Ishibashi, M. *Kobunshi Kagaku* **1958**, *15*, 619–627.
(12) Ziabicki, A. *Kolloid-Z.* **1959**, *167*, 132–141.
(13) Eppe, R.; Fischer, E. W.; Stuart, H. A. *J. Polym.Sci.* **1959**, *34*, 721–740.
(14) Keller, A.; Engleman, R. *J. Polym. Sci.* **1959**, *36*, 361–387.
(15) Geil, P. H. *J. Polym. Sci.* **1960**, *44*, 449–458.
(16) Roldan, L. G.; Kaufman, H. S. *J. Polym. Sci., Polym Lett.* **1963**, *1*, 603–608.
(17) Ogawa, M.; Ōta, T.; Yoshizaki, O.; Nagai, E. *J. Polym. Sci., Polym Lett.* **1963**, *1*, 57–61.
(18) Arimoto, H.; Ishibashi, M.; Hirai, M.; Chatani, Y. *J. Polym. Sci., Part A* **1964**, *2*, 2283–2295.
(19) Arimoto, H.; Ishibashi, M.; Hirai, M.; Chatani, Y. *J. Polym. Sci., Part A* **1965**, *3*, 317–326.
(20) Nagai, E.; Ogawa, M. *J. Polym. Sci., Polym Lett.* **1965**, *3*, 295–300.
(21) Miyasaka, K.; Makishima, K. *J. Polym. Sci., Part A-1* **1967**, *5*, 3017–3027.
(22) Parker, J. P.; Lindenmeyer, P. H. *J. Appl. Polym. Sci.* **1977**, *21*, 821–837.
(23) Simon, P.; Argay, G. Y. *J. Polym. Sci., Polym. Phys. Ed.* **1978**, *16*, 935–937.
(24) Stepaniak, R. F.; Garton, A.; Carlsson, D. J.; Wiles, D. M. *J. Polym Sci., Polym. Phys. Ed.* **1979**, *17*, 987–999.
(25) Kyotani, M. *J. Polym. Sci., Polym. Phys.* **1979**, *17*, 103–114.
(26) Heuvel, H. M.; Huisman, R. *J. Appl. Polym. Sci.* **1981**, *26*, 713–732.
(27) Gianchandani, J.; Spruiell, J. E.; Clark, E. S. *J. Appl. Polym. Sci.* **1982**, *27*, 3527–3551.
(28) Avramova, N.; Fakirov, S. *Polym. Commun.* **1984**, *25*, 27–29.
(29) Murthy, N. S.; Aharoni, S. M.; Szollosi, A. B. *J. Polym. Sci., Polym. Phys. Ed* **1985**, *23*, 2549–2565.
(30) Kiho, H.; Miyamoto, Y.; Miyaji, H. *Polymer* **1986**, *27*, 1542–1546.
(31) Murthy, N. S.; Minor, H.; Latif, R. A. *J. Macromol. Sci.: Phys. B* **1987**, *26*, 427–446.
(32) Murthy, N. S.; Minor, H. *Polym. Commun.* **1991**, *32*, 297–300.
(33) Murthy, N. S. *Polym. Commun.* **1991**, *32*, 301–305.
(34) Cai, W. W.; Li, C. Y.; Li, L. Y.; Lotz, B.; Keating, M.; Marks, D. *Adv. Mater.* **2004**, *16*, 600–605.
(35) Kyotani, M.; Mitsuhashi, S. *J. Polym. Sci. Part A-2* **1972**, *10*, 1497–1508.
(36) Gianchandani, J.; Spruiell, J. E.; Clark, E. S. *J. Appl. Polym. Sci.* **1982**, *27*, 3527–3551.
(37) Khanna, Y. P.; Reimschuessel, A. C. *J. Appl. Polym. Sci.* **1988**, *35*, 2259–2268.
(38) Khanna, Y. P.; Reimschuessel, A. C.; Banerjie, A.; Altman, C. *Polym. Eng. Sci.* **1988**, *28*, 1600–1606.
(39) Khanna, Y. P.; Kumar, R.; Reimschuessel, A. C. *Polym. Eng. Sci.* **1988**, *28*, 1607–1611.
(40) Khanna, Y. P.; Reimschuessel, A. C.; Banerjie, A.; Altman, C. *Polym. Eng. Sci.* **1988**, *28*, 1612–1615.
(41) Ramesh, C.; Gowd, E. B. *Macromolecules* **2001**, *34*, 3308–3313.
(42) Pei, A. H.; Liu, A. D.; Xie, T. X.; Yang, G. S. *Macromolecules* **2006**, *39*, 7801–7804.
(43) Crespy, D.; Landfester, K. *Macromol. Chem. Phys.* **2007**, *208*, 457–466.
(44) Huang, L.; Allen, E.; Tonelli, A. E. *Polymer* **1999**, *40*, 3211–3221.
(45) Wei, M.; Davis, W.; Urban, B.; Song, Y. Q.; Porbeni, F. E.; Wang, X. W.; White, J. L.; Balik, C. M.; Rusa, C. C.; Fox, J.; Tonelli, A. E. *Macromolecules* **2002**, *35*, 8039–8044.
(46) Yamauchi, K.; Kuroki, S.; Ando, I. *Polymer* **2002**, *43*, 3331–3333.
(47) Jones, N. A.; Atkins, E. D. T.; Hill, M. J.; Cooper, S. J.; Franco, L. *Polymer* **1997**, *38*, 2689–2699.
(48) Atkins, E. D. T.; Hill, M. J.; Hong, S. K.; Keller, A.; Organ, S. *Macromolecules* **1992**, *24*, 917–924.
(49) Jones, N. A.; Atkins, E. D. T.; Hill, M. J.; Cooper, S. J.; Franco, L. *Macromolecules* **1996**, *29*, 6011–6018.
(50) Navarro, E.; Alemán, C.; Subirana, J. A.; Puiggaí, J. *Macromolecules* **1996**, *29*, 5406–5415.
(51) Park, J. B.; Devries, K. L.; Statton, W. O. *J. Macromol. Sci., Phys., B* **1978**, *15*, 229–256.
(52) Samon, J. M.; Schultz, J. M.; Wu, J.; Hsiao, B. S.; Yeh, F.; Kolb, R. *J. Polym. Sci., Polym. Phys. Ed.* **1999**, *37*, 1277–1287.
(53) Schultz, J. M.; Hsiao, B. S.; Samon, J. M. *Polymer* **2000**, *41*, 8887–8895.
(54) Samon, J. M.; Schultz, J. M.; Hsiao, B. S. *Polymer* **2002**, *43*, 1873–1875.
(55) Huang, B. G.; Tao, D. L.; Xu, Y. Z.; Wang, J. J.; Weng, S. F.; Guo, J.; Wu, J. G.; Xu, D. F.; Xu, G. X. *Spectrosc. Spectr. Anal.* **2003**, *23*, 506–508.
(56) Kang, N.; Xu, Y. Z.; Wu, J. G.; Feng, W.; Weng, S. F.; Xu, D. F. *PCCP* **2000**, *2*, 3627–3630.
(57) Zhu, L.; Calhoun, B. H.; Ge, Q.; Quirk, R. P.; Cheng, S. Z. D.; Thomas, E. L.; Hsiao, B. S.; Yeh, F.; Liu, L.; Lotz, B. *Macromolecules* **2001**, *34*, 1244–1251.
(58) Sun, W. X.; Hu, X. B.; Xu, Y. Z.; Qu, L. W.; Yang, Z. L.; Wang, D. J.; Liu, X. X.; Guo, F. X.; Weng, S. F.; Wu, J. G.; Xu, D. F. *Acta Chim. Sin.* **2000**, *58*, 1602–1607.
(59) Keller, A. *Rep. Prog. Phys.* **1968**, *31*, 623–703.

MA8019333